J Ther Eng, Vol. 9, No. 6, pp. 1442−1451, November, 2023

Journal of Thermal Engineering
Web page info: https://jten.yildiz.edu.tr
DOI: 10.18186/thermal.1396640

Journal of Thermal Engineering

Research Article

Single-phase and two-phase models of a hybrid nanofluid traveling through a non-uniformly heated (PTC) receiver: A comparative study

Amina BENABDERRAHMANE[1], Ahmed Kadhim HUSSEIN[2], Obai YOUNIS[3,4,*], Abdelylah BENAZZA[5]

[1]*Department of Mechanical Engineering, Faculty of Sciences and Technology, University Mustapha Stambouli of Mascara, 90407, Algeria*
[2]*Department of Mechanical Engineering, College of Engineering, University of Babylon, 51002, Iraq*
[3]*Department of Mechanical Engineering, College of Engineering in Wadi Alddwasir, Prince Sattam Bin Abdulaziz University, 16273, Saudi Arabia*
[4]*Department of Mechanical Engineering, Faculty of Engineering, University of Khartoum, 11115, Sudan*
[5]*Faculty of Technology, Djilali Liabes University, Sidi Bel Abbes, 22000, Algeria*

ARTICLE INFO

Article history
Received: 15 September 2021
Revised: 27 September 2021
Accepted: 01 January 2022

Keywords:
CFD; Forced Convection; Parabolic Trough Solar Collector; Hybrid Nanofluid; Two-Phase Modeling; Turbulent Flow

ABSTRACT

The current study used single and two-phase modeling to numerically explore three-dimensional the turbulent forced convection of a hybrid nanofluid passing through a non-uniformly heated parabolic trough solar collector (PTC) for increasing heat transfer. The typical heat flux profile on the receiver's absorber outer wall was addressed by a finite volume method (FVM) and the MCRT method. The results demonstrated that the single and two-phase models produced almost similar hydrodynamic results but dissimilar thermal ones. It was found that the results of mixture model matched the experimental ones. The results also illustrated that the hybrid nanofluid gives the highest thermal performance for a mixture composed of 1.5% copper + 0.5% alumina dispersed in the water.

Cite this article as: Benabderrahmane A, Hussein AK, Younis O, Benazza A. Single-phase and two-phase models of a hybrid nanofluid traveling through a non-uniformly heated (PTC) receiver: A comparative study. J Ther Eng 2023;9(6):1442−1451.

INTRODUCTION

Recently, nanotechnology has facilitated the development of a new category of fluids known as nanofluids. It was composed of nanoparticles suspended in a fluid base. Nanofluids have intriguing characteristics that could make them suitable for a variety of engineering applications, such as heat transmission enhancement. Among other properties, nanofluids exhibit a significant enhancement in liquid thermal conductivity, liquid viscosity, and heat transfer coefficient. As is commonly known [1], metals in the solid state have higher thermal conductivities than liquids. Copper's thermal conductivity at ambient temperature is 700 times greater than that of water and 3000 times greater than engine oil. Metallic liquids have substantially

***Corresponding author.**
*E-mail address: oubeytaha@hotmail.com, o.elamin@psau.edu.sa

This paper was recommended for publication in revised form by Regional Editor Emre Alpman

greater thermal conductivity than nonmetallic liquids. Consequently, fluids containing suspended metal particles are predicted to have a substantially greater thermal conductivity than unadulterated liquids [2]. Two forms of nanofluid convective heat transfer modeling exist in general. The first is known as single-phase modeling, in which both the nanoparticles and the base fluid are considered homogeneous and to possess unique properties, taking into account the liquid and solid properties; the second is known as two-phase modeling, in this case the nanoparticles and the base fluid are treated independently. Alternatively, the solar collector, also known as a green heat exchanger device that converts solar energy into thermal energy in solar thermal applications or directly into electrical energy in PV (photovoltaic) applications [3-5], is one of the primary components of a solar energy and water heating system.

The parabolic trough solar collector (PTC) is one of the most crucial solar collector types. This variety of solar collector is a linear concentrating solar collector capable of operating between 15 and 400 degrees Celsius. Using the reflective surface of a linear parabolic reflector, it concentrates solar energy into a vacuum-sealed, tubular receiver located along the focal line of the parabola.

In the receiver, an interior absorber tube is enclosed by an exterior glass cover and supporting structures [6-7]. This type can be used to generate electricity or operate machinery. Sokhansefatetal [8] investigated the effect of Al_2O_3/synthetic oil nanofluid on heat transfer in a PTC tube. It was determined that raising the nanoparticle concentration and operating temperature improved heat transfer. Risi et al. [9] researched the thermal heat improvement for CuO+Ni/nitrogen gas-phase nanofluid in a transparent PTC tube. They demonstrated that upon 0.3% vol., the negative influence of the pressure drop overcame the favorable impact of the thermal characteristics. Moreover, their optimizing method indicated that the maximal solar to thermal efficiency was equivalent to 62.5%. Moghari et al. [10] numerically investigated the laminar forced and natural convection inside a horizontally mounted annulus filled with Al_2O_3/water nanofluid by using the two-phase modeling. Both the inside and outside walls maintained a constant thermal flux. In addition, the effects of nanoparticle concentration, Grashof number, and heat flux ratio on the hydrodynamic and thermal properties were illustrated. A hybrid nanofluid, on the other hand, is a highly sophisticated kind of nanofluid that can be described as a mixture of base fluid (such as oil, water, polymer solutions, etc.) and two (or more) different types of composite nanoparticles suspended in a base fluid simultaneously [11]. Madhesh et al. [12] investigated experimentally the convective heat transmission and rheological properties of hybrid Cu-TiO_2 nanofluids. Conclusion: the convective heat transfer coefficient was improved by increasing the concentration of hybrid nanofluids and the Reynolds number. Also postulated was a correlation between the Nusselt number and the Reynolds number, the Prandtl number, and the hybrid nanofluid volume concentration. Otanicar et al. [12] investigated experimentally the effect of various nanofluids on the efficiency of micro-solar thermal collectors. Utilizing nanofluids as an absorption medium increased its effectiveness by up to 5 percent, as reported. Benabderrahmane et al. [13] investigated numerically the enhancement of heat transmission within a PTC absorber with longitudinal fins and nanofluids. In their endeavor, Al_2O_3, Cu, SiC, and C nanoparticles were utilized. The authors concluded that Cu nanoparticles significantly enhanced thermal transfer compared to other nanoparticles. Mwesigye and Meyer [14] investigated numerically the optimal thermal and thermodynamic performance of PTC receivers using various nanofluid concentration ratios. For silver/ Therminol VP-1, copper/ Therminol VP-1, and Al_2O_3/ Therminol VP-1 nanofluids, the thermal efficiency of the PTC was enhanced by 13.9%, 12.5%, and 7.2%, respectively. This increase was accomplished by increasing the volume fraction of nanoparticles from 0% to 6%. Coccia et al. [16] investigated experimentally the effect of different water-based nanofluids on PTC performance. With the use of (Fe_2O_3, SiO_2, TiO_2, ZnO, Al_2O_3, and Au) nanoparticles, various concentrations and temperatures were investigated. They concluded that using nanofluids did not significantly enhance the collector's efficacy. Rehan et al. [17] compared the efficacy of low concentration ratio solar PTC using pure water, Al_2O_3/ water, and Fe_2O_3/ water nanofluids in a recent experimental investigation. Their comparison employed various concentrations (0.2%, 0.25%, and 0.3%) and volume flow rates (1, 1.5, and 2 L/min). Al_2O_3/ water and Fe_2O_3/ water nanofluids increased thermal efficacy by approximately 13% and 11%, respectively, when compared to unadulterated water. Bellos and Tzivanidis [18] analyzed the thermal performance of a PTC operating with mono and hybrid nanofluids. They reported a mean improvement in thermal efficiency of approximately 4.25 percent. Benabderrahmane et al. [19] investigated numerically the three-dimensional turbulent forced convection of Al_2O_3 nanofluid within a non-uniformly heated PTC receiver with two longitudinal fins. They utilized single two-phase modeling to enhance thermal transfer. They discovered that the combination of nanofluid and two longitudinal fins improved heat transfer within the collector. It is evident from the aforementioned research that the usage of hybrid nanofluids enhanced the thermal efficacy of PTC. However, it is still necessary to examine the impact of various hybrid nanofluid types on the thermal efficacy of PTC. Using both single-phase and two-phase models, this study intends to examine the influence of turbulent forced convection on a hybrid nanofluid within a non-uniformly heated solar PTC receiver.

GEOMETRICAL MODEL

Fig. 1 shows the model considered in the current study that consists of a receiver of the PTC. The borosilicate glass and the steel were the materials used for the glass cover. The annular gap between them is treated as a vacuum at low values of the pressure and the ambient temperature. A hybrid nanofluid circulates inside the absorber. Table 1 lists

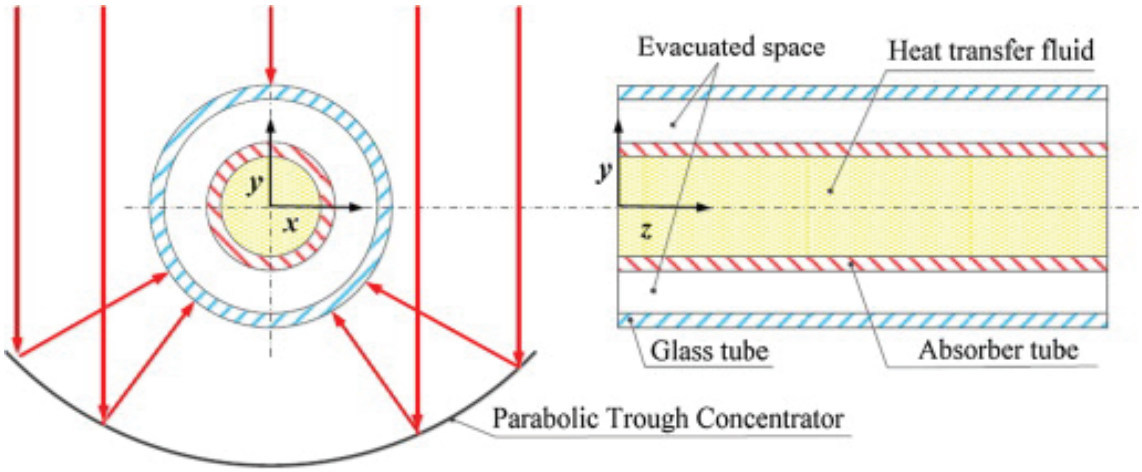

Figure. 1. Schematic of PTC receiver.

Table 1. Thermophysical properties of hybrid nanofluids.

	density (kg/m³)	Thermal capacity (J/kg K)	Thermal conductivity (W/m K)
Al_2O_3	3970	765	36
Cu	8954	383	400

Table 2. The physical parameters of the receiver

Length of the receiver	200 cm
The inner radius of the absorber	3.2 cm
The outer radius of the Absorber	3.5 cm
The inner radius of the glass cover	5.96 cm
The outer radius of the glass cover	6.25 cm
Absorber material	Steel
Glass envelope material	Borosilicate
The transmittance of the glass cover	96%
Coating absorbance	95%
Glass cover emissivity	0.873

the thermophysical characteristics of the nanofluid, while the dimensions of the receiver are listed in Table 2.

MATHEMATICAL MODEL

The governing equations of the mathematical model read:

- Continuity equation:

$$\nabla \cdot \rho \vec{V} = 0 \tag{1}$$

- Momentum equation:

$$\nabla \cdot \left(\rho \vec{V} \vec{V}\right) = -\nabla P + \nabla \cdot \left(\mu \nabla^2 \vec{V}\right) \tag{2}$$

- Energy equation:

$$\nabla \cdot \left(\rho \vec{V} C_p T\right) = \nabla \cdot \left(k \nabla T\right) - S_h \tag{3}$$

- Discrete Ordinate radiation model equation:

$$\frac{dI\left(\vec{r},\vec{s}\right)}{ds} + \left(a+\sigma_s\right) I\left(\vec{r},\vec{s}\right) = an^2 \frac{\sigma T^4}{\pi} + \frac{\sigma_s}{4\pi} \int_0^{4\pi} I\left(\vec{r},\vec{s'}\right) \Phi\left(\vec{s}\cdot\vec{s'}\right) d\Omega \tag{4}$$

- Turbulence model:

$$\frac{\partial k}{\partial t} + U_k \frac{\partial k}{\partial x_k} = \frac{\partial}{\partial x_k}\left[\left(\upsilon + \frac{C_\mu k^2}{\sigma_k \varepsilon}\right)\frac{\partial k}{\partial x_k}\right] + G_k + G_b - \varepsilon - Y_m + S_k \tag{5}$$

$$\frac{\partial \varepsilon}{\partial t} + U_k \frac{\partial \varepsilon}{\partial x_k} = \frac{\partial}{\partial x_k}\left[\left(\upsilon + \frac{C_\mu k^2}{\sigma_k \varepsilon}\right)\frac{\partial \varepsilon}{\partial x_k}\right] + C_{1\varepsilon}\frac{\varepsilon}{k}\left(G_k + C_{3\varepsilon} G_b\right) - C_{2\varepsilon}\frac{\varepsilon^2}{k} + S_\varepsilon \tag{6}$$

Where

$$G_k = -\rho \overline{u_i' u_k'} \frac{\partial U_k}{\partial x_k} = \mu_t S^2$$

$$G_b = \beta g_i \frac{\mu_t}{Pr_t}\frac{\partial T}{\partial x_i}$$

$$Y_M = 2\rho \varepsilon M_t^2$$

NUMERICAL METHOD

The finite volume method (FVM) is employed to accomplish the numerical simulation. The conventional

turbulence model k-ε was utilized. The pressure-based equation is solved using the pressure-based solver. The pressure and volume fraction are calculated using the PRESTO and QUICK methods. A second-order upwind approach is employed for the other convection-diffusion and radiation equations. A SIMPLE method is employed to address the pressure-velocity coupling. All the equations are solved sequentially and iteratively in order obtain a convergent solution. For all the simulations performed in this analysis, the convergence criteria are considered when the algebraic residuals are less than 10^{-4} for DO intensity, 10^{-6} for energy and epsilon equations and 10^{-3} for other equations.

GRID SENSITIVE STUDY

Table.3 shows the evolution of the average Nusselt number as a function of cell number for a range of Reynolds numbers between 10^4 and 10^6. A structured and refined mesh near the walls was used (Fig.2). A grid independence analysis is undertaken to limit the impact of the number of grid sizes on the obtained numerical results to justify the numerical findings' accuracy and stability.

BOUNDARY CONDITIONS

In this numerical investigation, the external wall of the absorber tube receives a non-uniform heat flux that was calculated using Monte-Carlo ray approach and a DNI value was assigned to be 1000 W/m2. Figure 3 illustrates the modeling outcomes of the local concentration ratio distribution on the outer absorber surface cross-section. The symmetry boundary condition is applied to annular space inlets and outlets. The envelope of the external glass implements a thermal boundary condition involving convective and radiative heat transfer. Sky temperature and emissivity are evaluated by the correlations given below [20, 21]:

$$T_{sky} = 0.0552 T_{amb}^{1.5} \tag{7}$$

$$\varepsilon_{sky} = 0.711 + 0.56\frac{T_{dp} - 273.15}{100} + 0.73\left(\frac{T_{dp} - 273.15}{100}\right)^2 \tag{8}$$

While the convective heat transmission coefficient is predicted by the subsequent experimental correlation **[22]**:

$$h_w = 4 v_w^{0.58} d_{go}^{-0.42} \tag{9}$$

MODEL VALIDATION

The Nusselt number and friction coefficient values for a simple tube were compared to those predicted using empirical correlations from the literature to attain confidence

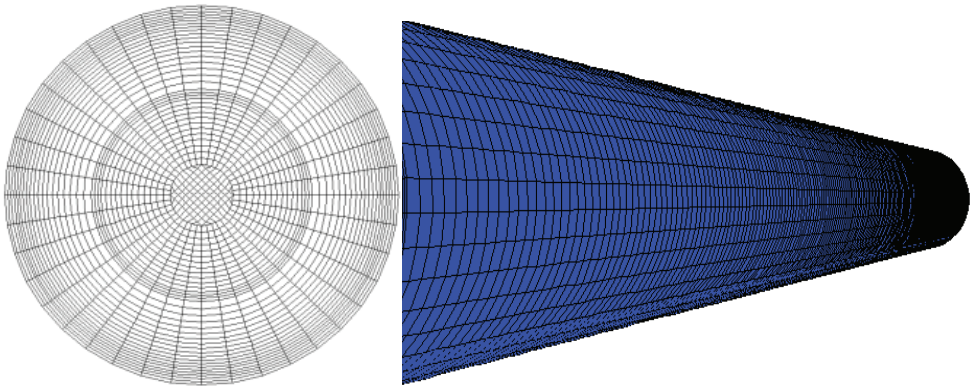

Figure 2. Geometry's mesh used in the study.

Table. 3. Mesh independence study

	N_{cells}				
	294600	307200	330400	354400	
Re	**Nu**				$\lvert\varepsilon_{max}\rvert$
10^4	208.123	210.021	209.613	211.461	**1.58%**
10^5	282.104	286.371	286.719	289.004	**3.39%**
10^6	319.121	318.223	319.942	320.781	**0.80%**

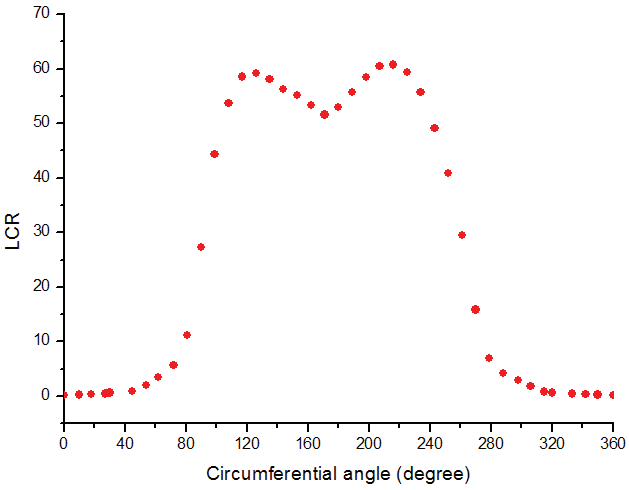

Figure 3. The local concentration ratio on a cross-section of the outer absorber surface.

about our numerical results. Gnielinski [23] proposed a correlation for estimating the Nusselt number inside turbulent tubes as a function of Reynolds number and Prandtl number, whereas the friction factor was calculated using Petukhov's correlation [24]. The correlations mentioned above are listed below:

$$Nu = \frac{\frac{f}{8}(Re-1000)Pr}{1+12.7\left(\frac{f}{8}\right)^{0.5}\left(Pr^{2/3}-1\right)} \quad (10)$$

$$f = \left(0.79\ln Re - 1.64\right)^{-2} \quad (11)$$

Ditus-Boelter [25] developed a straightforward formula for obtaining the Nusselt number using only the Reynolds and Prandtl numbers. This correlation is given by:

$$Nu = 0.023\,Re^{0.8}\,Pr^{n} \quad (12)$$

Where n = 0.4 when the wall temperature exceeds the bulk one, and n = 0.3 in the opposite case.

Blasius [26] recommended a correlation to calculate the friction factor inside smooth pipes under a turbulent flow as follow:

$$f = 0.316\,Re^{-0.25};\ Re \le 2\cdot 10^{4} \quad (13)$$

$$f = 0.184\,Re^{-0.2};\ Re > 2\cdot 10^{4} \quad (14)$$

Figure 4 indicates that the average Nusselt number and the friction factor are consistent, with the greatest variation being less than 8.5% and the minimum deviation being around 0.2%.

RESULTS AND DISCUSSION

Comparison Between Single and Two-Phase Models

The numerical analysis demonstrates that the local Nusselt number yields different values for homogeneous and two-phase models. Nonetheless, the calculations by the two-phase models are more accurate (Figure 5). In contrast, the local Darcy friction factor results are quite comparable (Fig. 6) when the maximum variation is approximately 2.7%. On the basis of Figures 5 and 6, it could be concluded that single and two-phase models generate nearly typical hydrodynamic behavior but dissimilar thermodynamic behavior.

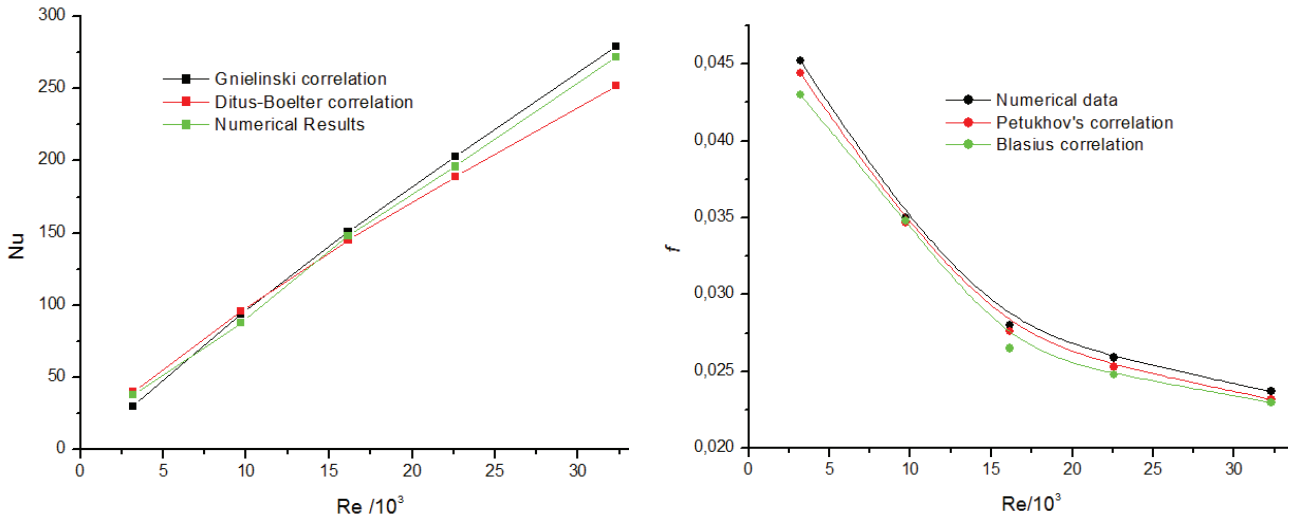

Figure. 4. Smooth pipe results validation.

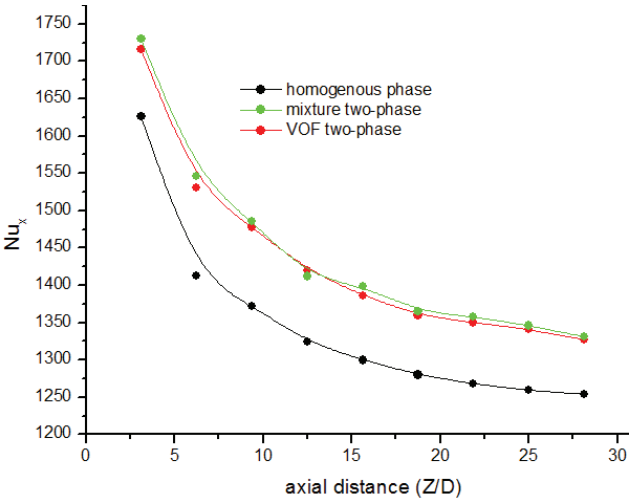

Figure 5. Local Nusselt number for single and two-phase models at Re = 36338; ϕ=0.01.

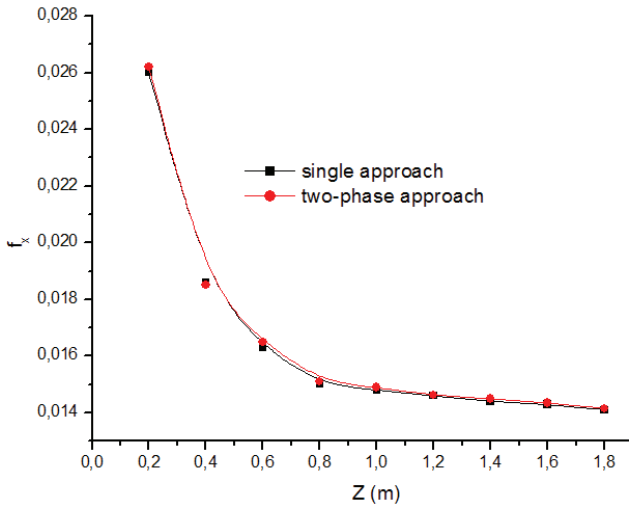

Figure 6. Local Darcy friction factor for single and two-phase models at Re= 36340 and ϕ=0.01.

Nusselt number values resulted from the simulations were compared against those values determined by the experimental correlations available in the literature for 1% alumina nanoparticles dispersed in water as the base fluid and under turbulent flow conditions in order to determine which model more closely matches the experimental results. In a tube, Xuan and Li [27] studied the nanofluid's flow and convective heat transfer. They proposed a correlation for calculating the average Nusselt number as a function of the Re, Pr, and Pe, in addition the nanoparticle volumetric fraction. These associations are demonstrated by:

$$Nu = 0.0059\left(1 + 7.628\phi^{0.6886} Pe_p^{0.001}\right) Re^{0.9238}\, Pr^{0.4} \qquad (15)$$

Where:

$$Pe_p = \frac{v\,d}{\alpha_{nf}} = \frac{v\,d\,\rho C_p}{\lambda}$$

In addition, **Velgapudi et al.** [28] suggested a correlation for the turbulent flow as a function of Re and Pr, which were given by:

$$Nu = 0.0256\, Re^{0.8} Pr^{0.4} \qquad (16)$$

Duangthongsuk and **Wongwises** [29] experimentally explored the coefficient of heat transmission and the friction factor for nanofluids confined inside a horizontally mounted tube. They established the correlation given below to predict the Nusselt number as a function Re and Pr together with the nanoparticle's concentration.

$$Nu = 0.074\, Re^{0.707} Pr^{0.385} \phi^{0.074} \qquad (17)$$

As shown in **Fig. 7,** the mixture model gives values closer to the experimental results, especially with the Nusselt number calculated by the correlation of Xuan and Li [27] where the maximum deviation did not exceed 5%; therefore, from these results, it may be concluded that the two-phase model is the most suitable for nanofluid flows. However, the homogenous model needs further modifications.

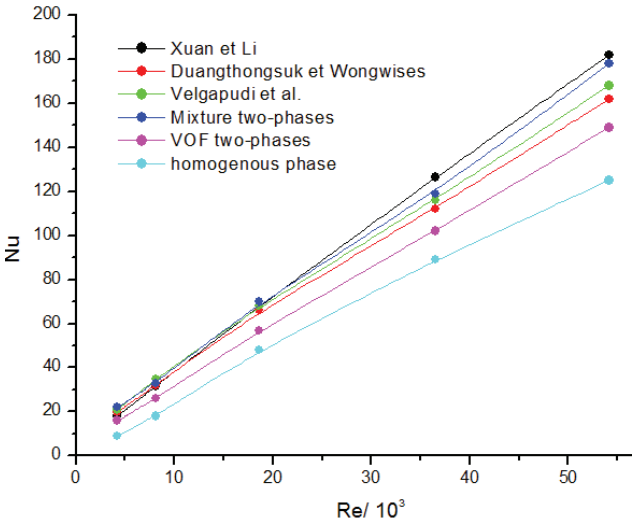

Figure 7. Single and two-phase models Vs. experimental data.

Impact of The Hybrid Nanofluid On Heat Transfer And Flow Field

Combining two distinct categories of dispersed nanoparticles in a base fluid is the most important characteristic of hybrid nanofluids. When nanoparticle materials are chosen properly, the positive characteristics of each can be enhanced, and the negative characteristics of a

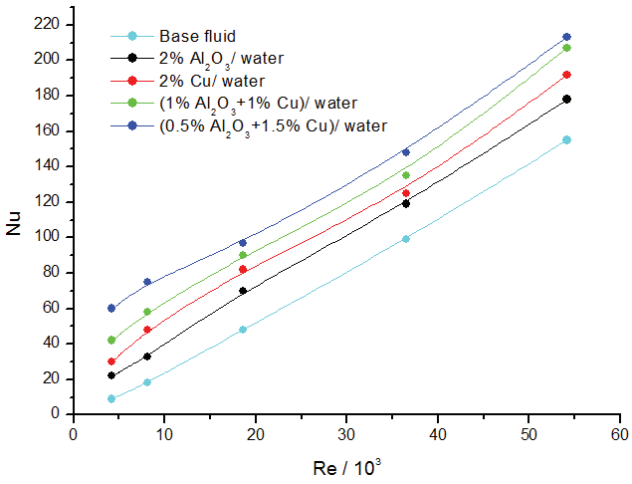

Figure 8. The impact of hybrid nanofluid on the heat transmission.

single material can be compensated for. Alumina, a ceramic material, possesses several advantageous properties, such as chemical inertness, strong corrosion resistance, and high stability. In contrast to metallic nanoparticles, its thermal conductivity is reduced. Nanoparticles of aluminum, zinc, copper, and other metals have a high thermal conductivity. In contrast, metallic nanoparticles have restricted applications in nanofluids due to their stability, reactivity, and high cost.

It is anticipated that the adding metal nanoparticles to a nanofluid composed of Al2O3 nanoparticles will improve the thermophysical characteristics of this composition, based on the properties of metallic and nonmetallic nanoparticles described above. Figure 8 depicts the fluctuation of the Nusselt number as a function of Re for various nanofluid solutions with a 2% volume fraction and 13 nanometer-diameter nanoparticles.

The findings indicate that the 2% (Cu+Al2O3)/water hybrid nanofluid possesses superior heat transmission properties in comparison to 2% copper or 2% alumina dispersed in water. The addition of metallic nanoparticles (Cu) to a nanofluid composed of water and oxide ceramic (Al2O3) is therefore predicted to substantially enhance the mixture's thermophysical properties and heat transfer characteristics.

In contrast, the addition of nanoparticles to water increases the Darcy friction factor, as shown in Fig. 9. This increase is likely due to an increase in HTF thermal conductivity. On the basis of the preceding analysis, it can be concluded that dispersing nanoparticles in water, which is used as the HTF within a PTC absorber, can improve heat transfer while simultaneously increasing the pressure drop within the absorber tube. Therefore, it is essential to calculate the thermal performance criteria (PEC), which could defined as the ratio between the dimensionless Nusselt number and the dimensionless friction factor:

$$PEC = \frac{Nu_i}{Nu_0} \sqrt[3]{\frac{f_0}{f_i}} \tag{18}$$

Figure 10 shows that the PEC value varies from 1.12 to 2.4, reflecting that the nanofluid offers a better comprehensive heat transfer enhancement than the base fluid. It is noted that the hybrid nanofluid improves the heat transmission greatly. This means that combining two different kinds of nanoparticles positively impacts the heat transfer characteristics.

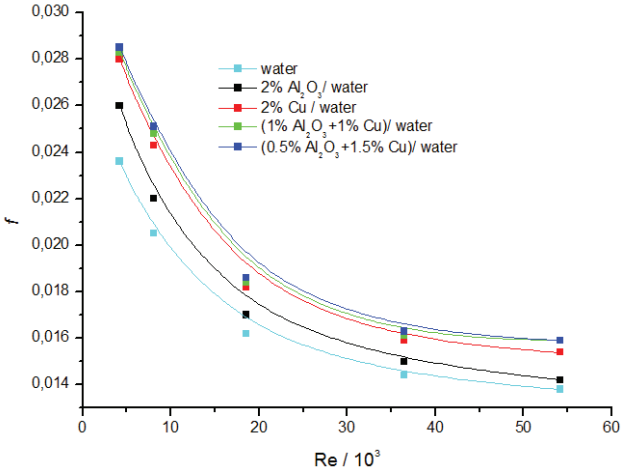

Figure 9. Effect of hybrid nanofluid on hydrodynamics characteristics.

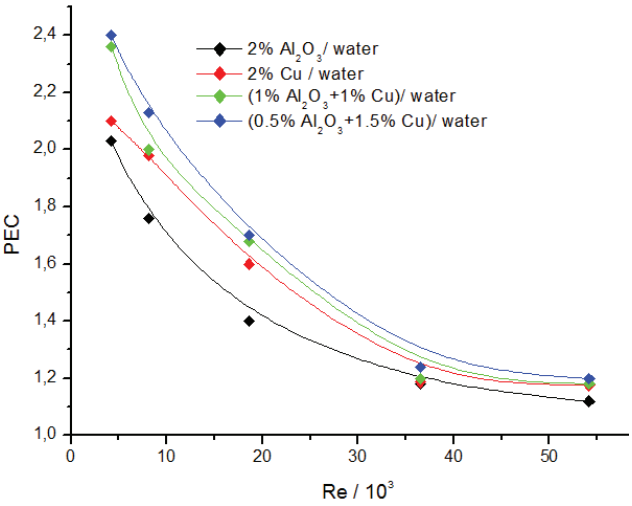

Figutre 10. Overall heat transfer performance of hybrid nanofluid.

Temperature Distribution Variation

Figures 11shows the distribution of temperature at the center cross-section of the absorber, the DNI was assigned to be 1000 W/m^2 and the inlet temperature of the HTF was

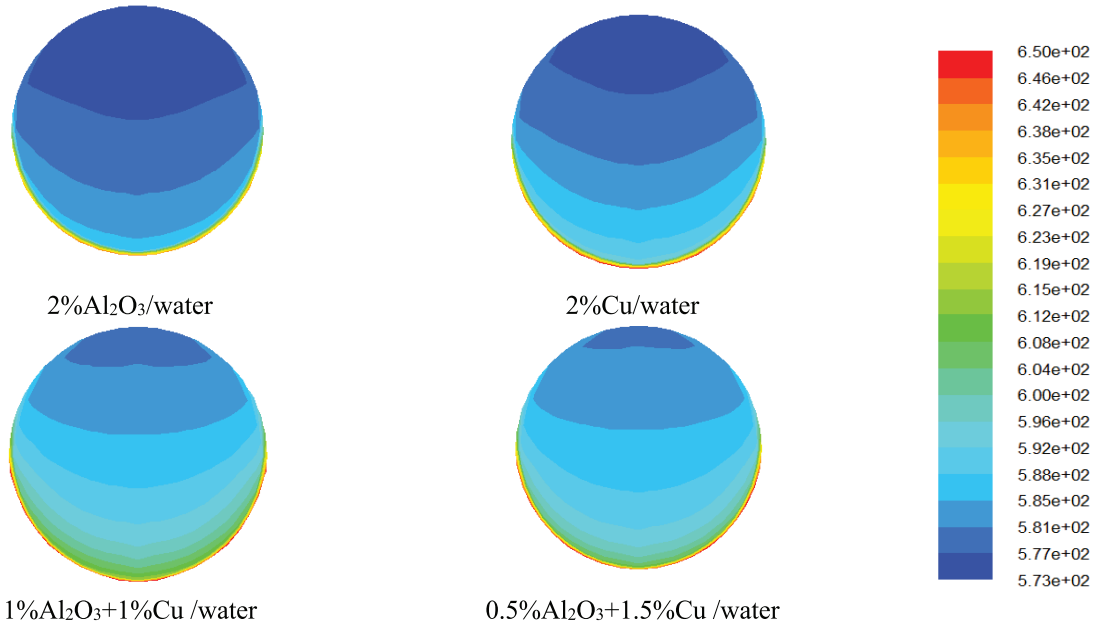

Figure 11. Temperature distribution (K) on the middle of the absorber (DNI= 1000 W/m^2 at HTF inlet temperature 573 K).

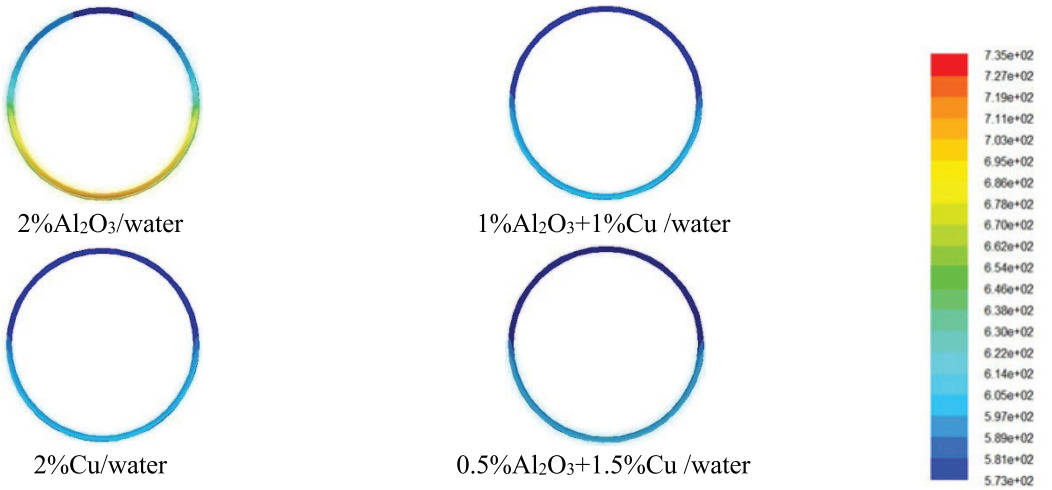

Figure 12. Temperature contours (K) at the middle cross-section of the absorber wall (DNI= 1000 W/m^2 at HTF inlet temperature 573 K)

573 K. It can be seen that the combination of the two different nanoparticles (Al_2O_3 and Cu) leads to increasing HTF temperature, this augmentation is due to dispersing the metallic particles, which have a higher thermal conductivity.

The temperature contours of the radial direction on the center cross-area of the absorber for the four nanofluids at the identical setting are showed in figure 12; the two-phase flow in the presence of Cu particles give remarkably almost identical values less than that obtained in the case of addition of Alumina particles; decreasing the temperature gradient affects an enhancement in the heat transfer coefficient.

CONCLUSION

Three dimensional numerical simulation of the turbulent forced convection of a hybrid nanofluid inside a PTC absorber was explored. The flow field was simulated employing the single and two-phase mixture and VOF models. The obtained findings demonstrate that single and two-phase models predict almost identical hydrodynamic results but dissimilar thermal ones, which means that the single-phase model still needs to be modified. The numerical results show that the hybrid nanofluid greatly augments the heat transfer characteristics, and it is considered better than the classical nanofluid. Moreover, it was found that

dispersing nanoparticles in water as a base fluid which is used as HTF inside a PTC absorber, can enhance the heat transfer, while it accompanies by enhancing the pressure drop in the absorber tube.

ACKNOWLEDGMENT

The Deanship of Scientific Research supported this publication at Prince Sattam bin Abdulaziz University, Alkharj, Saudi Arabia.

AUTHORSHIP CONTRIBUTIONS

Authors equally contributed to this work.

DATA AVAILABILITY STATEMENT

The authors confirm that the data that supports the findings of this study are available within the article. Raw data that support the finding of this study are available from the corresponding author, upon reasonable request.

CONFLICT OF INTEREST

The author declared no potential conflicts of interest with respect to the research, authorship, and/or publication of this article.

ETHICS

There are no ethical issues with the publication of this manuscript.

REFERENCES

[1] Bejan A, Kraus AD. Heat transfer handbook. Hoboken, NJ: John Wiley, Sons Inc; 2003.

[2] Choi SUS. Nanofluid technology: current status and future research. Vienna, VA United States: Korea-U.S. Technical Conference on Strategic Technologies; 1998.

[3] Hussein AK. Applications of nanotechnology in renewable energies-A comprehensive overview and understanding. Renew Sust Energ Rev 2015;42:460-76. [CrossRef]

[4] Hussein AK, Walunj AA, Kolsi L. Applications of nanotechnology to enhance the performance of the direct absorption solar collectors. J Therm Eng 2016;2:529-40. [CrossRef]

[5] Li D, Li Z, Zheng Y, Liu C, Hussein AK, Liu X. Thermal performance of a PCM-filled double-glazing unit with different thermophysical parameters of PCM. Sol Energy 2016;133:207-20. [CrossRef]

[6] Hussein AK. Applications of nanotechnology to improve the performance of solar collectors-Recent advances and overview. Renew Sust Energ Rev 2016;62:767-92. [CrossRef]

[7] Hussein AK, Li D, Kolsi L, Kata S, Sahoo B. A review of nanofluidrole to improve the performance of the heat pipe solar collectors. Energy Procedia 2017;109:417-24. [CrossRef]

[8] Sokhansefat T, Kasaeian AB, Kowsary F. Heat transfer enhancement in parabolic trough collector tube using Al2O3/ synthetic oil nanofluid. Ren Sust Energ Rev 2014;33:636-44. [CrossRef]

[9] Risi A, Milanese M, Laforgia D. Modelling and optimization of transparent parabolic trough collector based on gas-phase nanofluids. Ren Energ 2013;58:134-9. [CrossRef]

[10] Moghari RM, Akbarinia A, Shariat M, Talebi F, Laur R. Two-phase mixed convection Al2O3 /water nanofluid flow in an annulus. Int J Multipath Flow 2011;37:585-95. [CrossRef]

[11] Sarkar J, Ghosh P, Adil A. A review on hybrid nanofluids: recent research, development, and applications. Renew Sust Energ Rev 2015;43:164-77. [CrossRef]

[12] Madhesh D, Parameshwaran R, Kalaiselvam S. Experimental investigation on convective heat transfer and rheological characteristics of Cu-TiO2 hybrid nanofluids. Exp Therm Fluid Sci 2014;52:104-15. [CrossRef]

[13] Otanicar TP, Phelan PE, Prasher RS, Rosengarten G, Taylor RA. Nanofluid-based direct absorption solar collector. J Renew Sust Energ 2010;2:033102. [CrossRef]

[14] Benabderrahmane A, Aminallah M, Laouedj S, Benazza A, Solano JP. Heat transfer enhancement in a parabolic trough solar receiver using longitudinal fins and nanofluids. J Therm Sci 2016;25:410-7. [CrossRef]

[15] Mwesigye A, Meyer JP. Optimal thermal and thermodynamic performance of a solar parabolic trough receiver with different nanofluids and at different concentration ratios. Appl Energy 2017;193:393-413. [CrossRef]

[16] Coccia G, Di Nicola G, Colla L, Fedele L, Scattolini M. Adoption of nanofluids in low-enthalpy parabolic trough solar collectors: numerical simulation of the yearly yield. Energy Convers Manag 2016;118:306-19. [CrossRef]

[17] Rehan MA, Ali M, Sheikh NA, Khalil MS, Chaudhary GQ, Rashid T, et al. Experimental performance analysis of low concentration ratio solar parabolic trough collectors with nanofluids in winter conditions. Renew Energy 2018;118:742-51. [CrossRef]

[18] Bellos E, Tzivanidis C. Thermal analysis of parabolic trough collector operating with mono and hybrid nanofluids. Sustain Energy Technol Assess 2018;26:105-15. [CrossRef]

[19] Benabderrahmane A, Benazza S, Laouedj S, Solano J. Numerical analysis of compound heat transfer enhancement by single and two-phase models in parabolic trough solar receiver. Mechanika 2017;23:55-61. [CrossRef]

[20] Pandey DK, Lee RB, Paden J. Effects of atmospheric emissivity on clear sky temperatures. Atmos Environ 1994;29:2201-4. [CrossRef]
[21] García-Valladares O, Velázquez N. Numerical simulation of parabolic trough solar collector: improvement using counter flow concentric circular heat exchangers. Int J Heat Mass Transf 2009;52:597-609. [CrossRef]
[22] Mullick SC, Nanda SK. An improved technique for computing the heat loss factor of a tubular absorber. Sol Energy 1989;42:1-7. [CrossRef]
[23] Gnielinski V. New equations for heat and mass transfer in turbulent pipe and channel flow. Int J Chem Eng 1976;16:359-68.
[24] Petukhov BS. Heat transfer and friction in turbulent pipe flow with variable physical properties. Adv Heat Transf 1970;6:503-64. [CrossRef]
[25] Mills AF. Basic heat mass transfer. 2nd ed. New Jersey: Prentice-Hall; 1999.
[26] Incropera FP, Dewitt DP. Fundamentals of heat and mass transfer. 3rd ed. New York: John Wiley and Sons; 1990.
[27] Xuan Y, Li Q. Investigation on convective heat transfer and flow features of nanofluids. J Heat Transf 2003;125:151-5. [CrossRef]
[28] Vasu V, Rama KK, Chandra AKS. Empirical correlations to predict thermophysical and heat transfer characteristics of nanofluids." Therm Sci 2008;12:27-37. [CrossRef]
[29] Duangthongsuk W, Wongwises S. An experimental study on the heat transfer performance and pressure drop of TiO2-water nanofluids flowing under a turbulent flow regime. Int J Heat Mass Transf 2010;53:334-44. [CrossRef]

Appendix A

The VOF model is intended to monitor the position and movement of a free surface that exists between two or more fluids that are incompatible with one another. In this approach, the computation of any property involves finding the weighted average of many phases with respect to the volume fractions of those phases. The following are the definitions of the continuity, momentum, and energy equations:

$$\nabla\left(\phi_k \rho_k \vec{V}_k\right) = 0$$

where:

$$\sum_{k=1}^{n} \phi_k = 1$$

$$\rho \vec{V} \nabla \vec{V} = -\nabla P + \nabla\left(\mu \nabla \vec{V}\right) + \rho g$$

$$\nabla\left(\vec{V}\left(\rho E + P\right)\right) = \nabla\left(K \nabla T\right)$$

Appendix B

The mixing model is Eulerian technique that has been simplified, and it operates on the premise that the Stokes number is relatively low. The equation for the mixture's momentum as well as the equation for the volume fraction transport of each secondary phase are both solved by it. The following are the equations that define them:

$$\nabla\left(\rho_m \overrightarrow{V_m}\right) = 0$$

$$\nabla \cdot \sum_{k=1}^{n}\left(\rho_k C_{pk} \phi_k V_k T\right) = \nabla \cdot \left(K_m \nabla T\right)$$

$$\rho_m \overrightarrow{V_m} \nabla \overrightarrow{V_m} = -\nabla P_m + \left(\mu_m \nabla \overrightarrow{V_m}\right) + \rho_m g + \nabla\left(\sum_{k=1}^{n} \phi_k \rho_k \vec{V}_{dr,k} \vec{V}_{dr,k}\right) \vec{V}_{dr,k} = \vec{V}_k - \vec{V}_m$$

Velocity	Density	Viscosity
$\overrightarrow{V_m} = \frac{\sum_{k=1}^{n} \phi_k \rho_k V_k}{\rho_m}$	$\rho_m = \sum_{k=1}^{n} \phi_k \rho_k$	$\mu_m = \sum_{k=1}^{n} \phi_k \mu_k$

$$\nabla\left(\rho_p \phi_p \vec{V}_m\right) = -\nabla\left(\rho_p \phi_p \vec{V}_{dr,p}\right)$$

$$\vec{V}_{pf} = \frac{\tau_p d_p^2}{18 \mu_f f_{drag}} \frac{\rho_p - \rho_m}{\rho_p} \vec{a}$$

$$\text{Where } \vec{a} = \vec{g} - \left(\overrightarrow{V_m} \cdot \nabla\right) \vec{V}_m$$

$$\begin{cases} f_{drag} = 1 + 0.15\, Re_p^{0.687} & Re_p \leq 1000 \\ f_{drag} = 0.0183\, Re_p & Re_p > 1000 \end{cases}$$

$$Re_p = \frac{\rho_m V_m d_p}{\mu_m}$$